Clays and Clay Minerals, Vol. 52, No. 4, 399–410, 2004.

INTERPRETATION OF INFRARED SPECTRA OF DIOCTAHEDRAL SMECTITES IN THE REGION OF OH-STRETCHING VIBRATIONS

BELLA B. ZVIAGINA[1], DOUGLAS K. MCCARTY[2], JAN ŚRODOŃ[3] AND VICTOR A. DRITS[1]

[1] Geological Institute RAS, Pyzhevsky per. 7, Moscow, 119017, Russia
[2] ChevronTexaco Inc., 3901 Briarpark, Houston, TX 77042, USA
[3] Polish Academy of Sciences, Institute of Geological Sciences, Senacka 1, Krakow 31-002, Poland

Abstract—Dioctahedral smectite samples of a wide range of compositions (beidellites, montmorillonites, nontronites, Fe-rich montmorillonites and Al-rich nontronites) were studied by infrared (IR) spectroscopy. A special sample-preparation technique was used to eliminate the contribution of molecular water. The OH-stretching regions of the spectra were decomposed and curve-fitted, and the individual OH-stretching bands were assigned to all the possible types of OH-bonded cation pairs that involve Al, Mg and Fe. The integrated optical densities of the OH bands were assumed to be proportional to the contents of the specific types of OH-linked cation pairs with the absorption coefficients being the same for all individual OH bands. Good agreement between the samples' octahedral cation compositions calculated from the IR data and those given by crystal-chemical formulae was obtained for a representative collection of samples in terms of a unique set of individual OH-band positions that vary within narrow wavenumber intervals. This has allowed us to minimize the ambiguity in spectra decomposition caused by the poor resolution of smectite spectra and confirmed the validity of the resulting band identification.

The bands associated with specific OH-bonded cation pairs in the spectra of smectites are, on the whole, shifted to greater wavenumbers with respect to the corresponding bands in micas. In addition to OH bands that refer to the smectite structure, AlOHAl and AlOHFe bands of the pyrophyllite structural fragments were identified. The band-position variation ranges overlap in a few cases (AlOHFe and MgOHMg; AlOHAl of smectite and AlOHFe of pyrophyllite-like component).

Unambiguous interpretation of the OH-stretching vibrations was found to be possible only for smectite samples with known chemical compositions, so that IR data cannot be used for quantitative determination of octahedral cation composition of mixtures of dioctahedral 2:1 phyllosilicates. In the case of the studied monomineral smectites with known chemical compositions, IR data provided information on the short-range order/disorder in the distribution of octahedral cations along cation-OH-cation directions. This information can be employed, in conjunction with the data of other spectroscopic and diffraction techniques, in the analysis of short-range octahedral cation distribution.

Key Words—Cation Distribution, Dioctahedral Smectite, IR Spectroscopy, OH-stretching Vibrations, Short-range Order/Disorder.

INTRODUCTION

One of the basic problems in the determination of the actual crystal structure of dioctahedral 2:1 phyllosilicates is the reconstruction of the two-dimensional cation distribution patterns in terms of both short-range and long-range cation ordering. Whereas diffraction methods provide information on long-range cation order/disorder, various spectroscopic methods are sensitive to local atomic environments and therefore have a potential for determining short-range ordering in the cation distribution. Infrared (IR) spectroscopy has proven an effective tool for the determination of local atomic arrangements and fine structural features. Specifically, hydroxyl IR vibrations probe local cation environments around OH groups and therefore can be used for the determination of the types and amounts of octahedral cations coordinated to hydroxyls and the patterns in the cation distribution (Farmer and Russell, 1964; Farmer, 1974; Russell and Fraser, 1994; Besson and Drits 1997a, 1997b).

Interpretation of IR spectra of dioctahedral 2:1 phyllosilicates in the region of OH vibrations is a fundamental problem that has been studied by numerous authors (*e.g.* Farmer, 1974 and references therein; Besson and Drits, 1997a, 1997b and references therein; Decarreau *et al.*, 1992; Madejová *et al.*, 1992, 1994; Petit *et al.*, 1995, 2002; Cuadros and Altaner, 1998; Vantelon *et al.*, 2001; Fialips *et al.*, 2002a, 2002b; Gates *et al.*, 2002; Gates, 2003). Developing the methodology of Slonimskaya *et al.* (1986), Besson and Drits (1997a, 1997b) suggested a new model for the interpretation of IR spectra of dioctahedral micas within the OH-stretching region. They applied a sophisticated decomposition and curve-fitting procedure to IR spectra of dioctahedral mica samples with known and diverse chemical compositions. The integrated optical densities of the OH bands were assumed to be proportional to the contents of the specific types of OH-linked cation pairs

* E-mail address of corresponding author:
zviagina@ginras.ru
DOI: 10.1346/CCMN.2004.0520401

Copyright © 2004, The Clay Minerals Society

https://doi.org/10.1346/CCMN.2004.0520401 Published online by Cambridge University Press

with the absorption coefficients being the same for all individual OH bands. As a result, Besson and Drits (1997a, 1997b) provided unambiguous assignments of the band positions to each type of OH-bonded cation pair.

Attempts have been made to apply a similar approach to the interpretation of OH-stretching vibrations in the IR spectra of dioctahedral smectites (Madejová *et al.*, 1992, 1994; Fialips *et al.*, 2002a, 2002b; Petit *et al.*, 2002). For the most part, however, individual OH bands were assigned to specific cation pair types based on previous work without establishing any assignment rules. There have been significant uncertainties in the OH-band assignments. For example, the attribution of OH bands suggested by Fialips *et al.* (2002b) (in particular, for Al-rich nontronite SWa-1) contradicts that obtained by Madejová *et al.* (1994). Another serious complication to the interpretation of smectite IR spectra is the considerable contribution of molecular water vibrations, which overlaps with the low-wavenumber part of the OH-stretching region. Although several authors (Madejová *et al.*, 1992, 1994; Fialips *et al.*, 2002a, 2002b; Petit *et al.*, 2002) have minimized this water contribution using appropriate experimental techniques, there has been considerable ambiguity in the number and positions of the bands corresponding to H_2O.

The poor resolution of the individual OH bands characteristic of smectite spectra may lead to several decompositions of a single spectrum that would provide equally good agreement between the octahedral cation composition calculated from the IR data and that obtained by the crystal-chemical formula. The purpose of the present paper was therefore to analyze the OH-stretching regions of IR spectra for a representative collection of dioctahedral smectite samples of diverse compositions and to find such a set of individual OH-band positions attributed to specific cation pair types that would ensure good fit of cation compositions for all the samples. In this case, the agreement between the IR data on cation composition and the crystal-chemical formulae can serve as the criterion for the validity of the OH-band assignment.

MATERIALS AND METHODS

The crystal-chemical formulae of the smectite samples selected for the IR study, as well as their source localities are given in Table 1. According to the chemical composition, these smectites can be divided into four groups: (1) beidellites having almost purely aluminous octahedral cation composition (Nos. 1, 2); (2) relatively Mg-rich montmorillonites with low Fe contents (Nos. 3–6); (3) nontronites (Nos. 7, 8); (4) smectites having mixed cation compositions: Al-rich nontronites (Nos. 9, 10) and Fe-rich montmorillonites (Nos. 11–14).

Samples 1–6, 9–14 were not tested for the Fe(II)/Fe(III) ratio, and all Fe in these samples was assumed to be trivalent, also taking into account that Fe-rich smectites were shown experimentally to contain no noticeable Fe(II) (*e.g.* Fialips *et al.*, 2002a, 2002b). Samples 7 and 8 (nontronites 598 and 1092) contain only Fe(III) according to wet chemical analysis (Chekin, 1973).

In order to remove most of the molecular water from the smectite samples, a special sample-preparation procedure was used. After treatment with Na acetate

Table 1. Cation compositions of smectites under study (atoms per $O_{10}(OH)_2$).

		Interlayer					Tetrahedra		Octahedra		
	Sample[†]	Na	Ca	Sr	K	Mg	Si	Al	Al	Fe	Mg
1	BJ, Black Jack Mine, Idaho	0.48	0.01			0.01	3.48	0.52	1.98	0.02	
2	BT, Blaine Tunnel	0.37					3.64	0.36	1.87	0.09	0.04
3	Otay, California	0.12	0.35				3.92	0.08	1.18	0.08	0.74
4	Polkville, Missisipi	0.18	0.21				3.90	0.10	1.42	0.08	0.50
5	Montmorillon, France		0.23				3.87	0.13	1.65	0.04	0.30
6	SAz-1, Cheto, Arizona	0.48	0.04				4.00		1.36	0.08	0.56
7	598, Olkhon, Siberia	0.04	0.12			0.02	3.59	0.41	0.35	1.68	
8	1092, Olkhon, Siberia	0.05	0.12			0.17	3.44	0.56	0.33	1.60	0.07
9	SWa-1a, Washington	0.46					3.68	0.32	0.64	1.22	0.14
10	SWa-1b, Washington	0.22					3.69	0.31	0.54	1.34	0.12
11	SWy-2, Wyoming	0.31	0.01				3.88	0.12	1.54	0.23	0.24
12	BF, Belle Fourche, South Dakota	0.35					3.87	0.13	1.58	0.20	0.22
13	JP, Jelsovy Potok, Slovakia	0.18					3.90	0.10	1.57	0.17	0.26
14	2M5, Upper Silesia, Poland	0.01	0.02	0.15	0.07		3.88	0.12	1.50	0.16	0.35

[†] 1–6, 9–12 – Source Clays Repository, The Clay Minerals Society; 9 and 10 are different fractions of the heterogeneous SWa-1 clay standard, <0.2 and 2.0 μm, respectively. Crystal-chemical formulae taken from: 2, 4, 12 – Foster (1953), 1, 3, 5, 6, 9 – Eberl *et al.*, (1986), 10, 11 – own chemical analysis data.
7, 8 – courtesy of S.S. Chekin (Chekin, 1973)
13 – courtesy of B. Čičel (Čičel and Komadel, 1994)
14 – collected by J. Środoń (Środoń *et al.*, 1986)

https://doi.org/10.1346/CCMN.2004.0520401 Published online by Cambridge University Press

and Na dithionite (Jackson, 1985) and centrifugation, the material was oven dried and then freeze dried using 100 mg of sample in 150 mL of distilled water (McCarty and Reynolds, 1995). A 5 mg portion of the freeze-dried material was combined with 95 mg of KBr and homogenized with the help of a Retsch®MM200 mixing mill. Then 40 mg of the mixture obtained were combined with 460 mg of KBr and homogenized. Then 200 mg of the resulting mixture were placed in a 13 mm pellet die and pressed under vacuum for 10 min. The pellet was placed into a vacuum oven and heated at 185ºC for at least 14 h and then cooled for 30 min in a desiccant box. After cooling, the IR spectra were recorded using a Nicolet ESP-260 spectrometer within the 300–4000 cm^{-1} range, with a 4 cm^{-1} resolution. The IR absorbance conversion was made automatically with the Nicolet®Omnic Software Version 5.0.

The OH-stretching region of each spectrum (3200–3750 cm^{-1}) was baseline-corrected, decomposed and fitted using the Galactic PeakSolve™ program. Although theoretically the vibrational bands should be Lorentzian, various instrumental and/or compositional factors affect their shape leading to a Gaussian or mixed Gaussian-Lorentzian distribution (Strens, 1974). For the IR spectra under study, the best fitting results were obtained assuming a symmetric Gaussian peak shape for each OH band. The variable parameters were position, width at half-height, and intensity of each component; the widths at half-height of the individual bands in a spectrum did not differ by more than 20%. The complex wide absorption band of the residual water was included in the fitted spectrum as two broad maxima around 3200 and 3420 cm^{-1}. The actual positions of the individual bands comprising the molecular water contribution will be discussed below. The quality of spectra decomposition was estimated by the minimization function, χ^2, and the correlation coefficient, R, as well as by the agreement between the experimental spectrum profile with that synthesized by summation of the extracted individual bands. The integrated optical densities were assumed to be proportional to the areas of the corresponding peaks, with equal absorption coefficients for all cation pair types. Octahedral cation composition could be thus calculated from the IR data and compared with that given by the crystal-chemical formula, which served as a criterion for the choice of the number of individual components in the fitted spectrum. If two or more solutions gave satisfactory fits of cation composition, the solution with the best χ^2 was chosen.

RESULTS

The individual OH-band positions assigned to specific cation pair types, as obtained from decomposition of the IR spectra of the smectites are given in Table 2. Table 3 gives the relative integrated intensities of the OH bands. Selected decomposed and fitted spectra are shown in Figures 1–6. The experimental and the calculated curves overlapped without any visible differences, so that the calculated curves are not shown.

The IR spectra of beidellites BJ (Figure 1) and BT contain three intense bands at ~3628, 3652 and 3670 cm^{-1} and a weaker band at 3696–3698 cm^{-1}, which were interpreted as AlOHAl-stretching vibrations. The two higher-frequency bands of these four may be associated with the presence of pyrophyllite-like local structural fragments (see below). Beidellite BT shows a band at 3608 cm^{-1} identified as AlOHMg. In addition,

Table 2. Positions of OH-stretching bands (cm^{-1}) corresponding to specific OH-bonded cation pairs and molecular water bands as obtained from the decomposition of IR spectra.

Band	1	2	3	4	5	6	7	8	9	10	11	12	13	14
Sample														
FeOHFe						3543	3536	3534	3540	3539				
FeOHFe		3562	3552				3550	3552	3562	3558		3558	3558	
FeOHFe				3566	3573		3570	3572	3579	3580	3572			
MgOHFe												3581	3579	3580
MgOHMg			3590	3591	3586	3585								
AlOHFe	3595	3594					3586	3589	3596	3594		3594		
AlOHMg		3608	3609	3607	3606	3604		3612	3613	3611	3601	3608	3601	3603
AlOHAl	3628	3630	3631	3630	3626	3626	3620	3634	3632	3629	3630	3625	3625	3630
AlOHAl	3652	3652	3652	3657	3646	3652			3657		3656	3644	3648	3652
Pyr.-like:														
AlOHFe										3649	3656	3660	3648	3652
AlOHAl	3671	3670	3670		3668	3678						3678	3677	3675
AlOHAl	3698	3696	3684	3691	3691				3690	3688	3692	3693	3703	3699
$(H_2O)1$	3205	3185	3234	3256	3196	3233	3226	3229	3214	3226	3249	3233	3262	3232
$(H_2O)2$	3432	3425	3425	3430	3420	3425	3431	3435	3430	3440	3429	3425	3430	3432
$\chi^{2\dagger}$	0.78	2.28	2.82	2.39	1.55	6.38	0.88	2.59	4.28	3.93	2.24	4.86	5.82	1.95

† minimization function

https://doi.org/10.1346/CCMN.2004.0520401 Published online by Cambridge University Press

Table 3. Relative integrated intensities (%) of OH-stretching bands corresponding to specific OH-bonded cation pairs.

Band	1	2	3	4	5	6	7	8	9	10	11	12	13	14
Sample														
FeOHFe							24.6	18.9	24.4	11.8				
FeOHFe			2.6			2.7	23.2	27.9	19.6	24.0				
FeOHFe		3.0		5.6	1.6		28.5	24.4	12.8	20.3	2.5	1.2	1.6	
MgOHFe												5.4	4.1	6.2
MgOHMg			22.1	15.3	4.6	17.9								
AlOHFe	4.2	10.8					18.1	17.1	11.7	7.7		7.4		
AlOHMg		7.4	26.3	17.6	17.5	20.0		8.1	13.0	13.5	27.9	14.0	20.7	25.0
AlOHAl	37.55	41.6	25.0	31.1	17.2	32.6	5.8	3.5	10.6	7.8	36.3	25.3	29.7	34.7
AlOHAl	15.05	12.4	8.6	20.9	34.7	15.5			6.4		4.9	25.5	15.0	7.2
Pyr.-like:														
AlOHFe										12.8	18.0	9.0	10.0	9.0
AlOHAl	38.8	20.4	7.2		11.1	11.3						1.8	14.2	10.3
AlOHAl	4.4	6.7	8.2	9.5	13.2				1.4	2.1	10.4	10.0	4.7	7.6

the spectra of these beidellites contain weak AlOHFe bands (3595 cm^{-1}) and, in the case of BT, an FeOHFe band at 3562 cm^{-1} that corresponds to the low Fe contents in the samples.

The spectra of montmorillonites with relatively high Mg and low Fe contents (Polkville, Figure 2, Otay, SAz-1, Montmorillon, France), in addition to AlOHAl and AlOHMg vibrations, show a low-intensity FeOHFe band and a strong band at 3585–3591 cm^{-1} (Tables 2, 3), which was attributed to the MgOHMg vibration. It is noteworthy that there are no other bands that could be associated with the high Mg content in these samples. MgOHMg-stretching bands were reported previously by Besson and Drits (1997a) for the IR spectra of dioctahedral micas.

The IR spectra of nontronites 598 (Figure 3) and 1092 and Al-rich nontronites SWa-1a and SWa-1b (Figure 4) show three FeOHFe bands (Tables 2, 3). The IR spectra of these samples also contain AlOHFe, AlOHMg (except 598) and AlOHAl bands.

In the spectrum of Al-rich nontronite SWa-1b, the band at 3649 cm^{-1} was attributed to the AlOHFe vibration in the pyrophyllite-like structural fragments, as it is close to the position of the AlOHFe-stretching band (3647 cm^{-1}) in pyrophyllite IR spectra (Farmer, 1974). These vibrations were also identified for all the studied Fe-rich montmorillonites (SWy-2 (Figure 5), JP (Figure 6), BF and 2M5, Table 2); in these cases, the band in question overlaps with one of the AlOHAl bands of smectite proper. The presence of pyrophyllite-like fragments in dioctahedral 2:1 phyllosilicates was reported by Besson and Drits (1997a, 1997b)

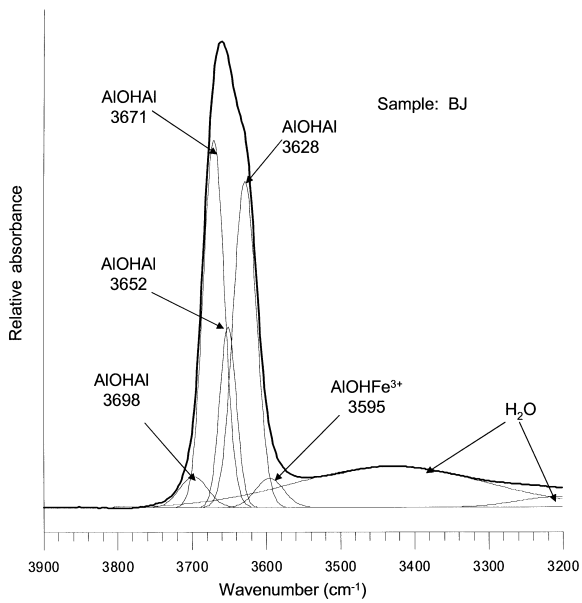

Figure 1. Decomposition of the IR spectrum of beidellite Black Jack Mine (BJ).

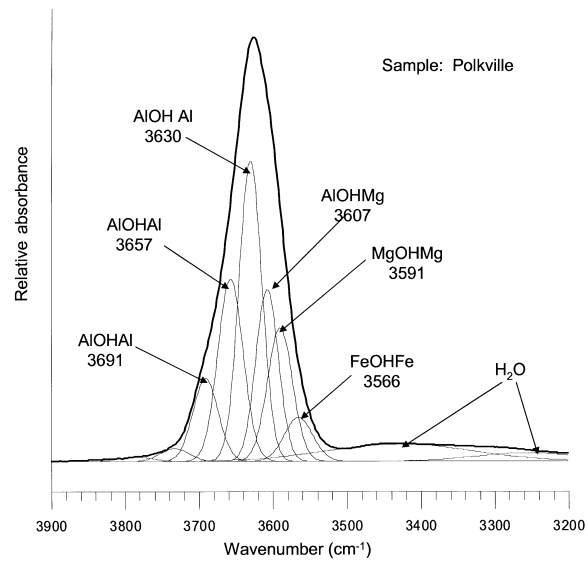

Figure 2. Decomposition of the IR spectrum of montmorillonite Polkville.

https://doi.org/10.1346/CCMN.2004.0520401 Published online by Cambridge University Press

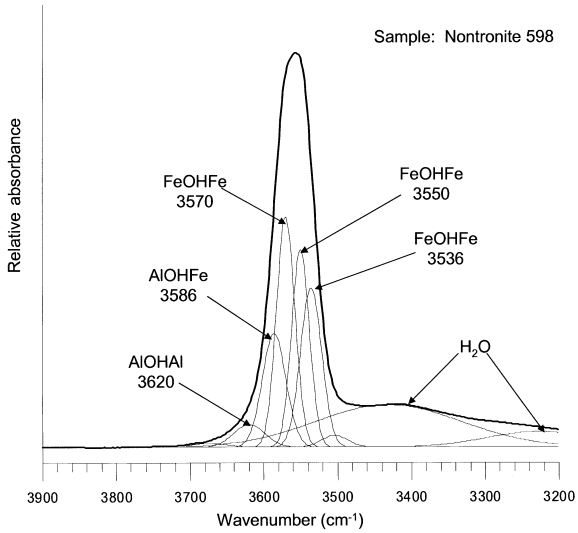

Figure 3. Decomposition of the IR spectrum of nontronite 598.

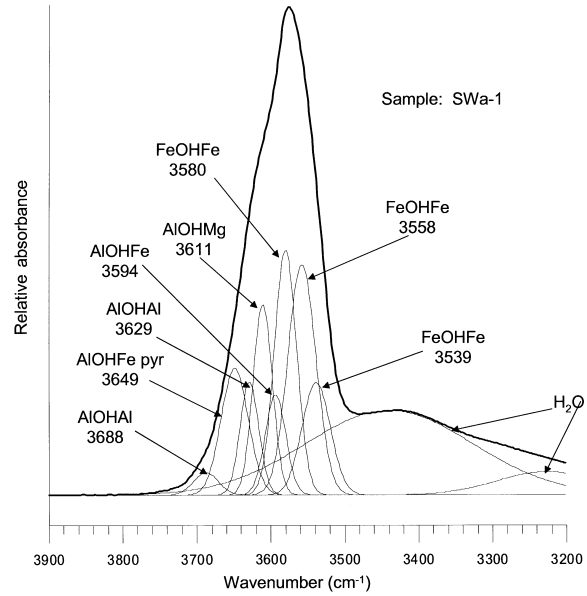

Figure 4. Decomposition of the IR spectrum of Al-rich nontronite SWa-1b.

who identified FeOHFe, AlOHFe and AlOHAl vibrations of the pyrophyllite-like component in the IR-stretching regions of celadonites, glauconites and illites.

Each spectrum of the Fe-rich montmorillonites also contains one FeOHFe band (except 2M5), an AlOHMg band and three or four AlOHAl bands, two of which refer to smectite proper and one or two presumably to the pyrophyllite-like local environments (Table 2). The band at ~3580 cm^{-1} present in the spectra of samples BF, JP (Figure 6) and 2M5 was attributed to MgOHFe vibration. Note that this vibration was identified only in these three samples, which have similar amounts of Fe and Mg. Taking account of the experimental error, the position of the MgOHFe band is fairly close to that found by Petit *et al.* (2002) for Ölberg Fe-rich montmorillonite (3575 cm^{-1}).

The minor bands observed in the high-wavenumber region in some of the spectra (*e.g.* Figure 2) could be artifacts resulting from the use of strictly Gaussian peak shape. Their contributions are, however, negligible and have not been included in the spectra decomposition.

The resulting OH-band assignments are summarized in Table 4, which shows the mean band positions that refer to specific OH-bonded cation pairs, as well as the corresponding estimated standard deviations (esd). In comparison with mica spectra (Besson and Drits, 1997a), the individual OH-stretching band positions in the spectra of smectites vary within wider ranges (esds are

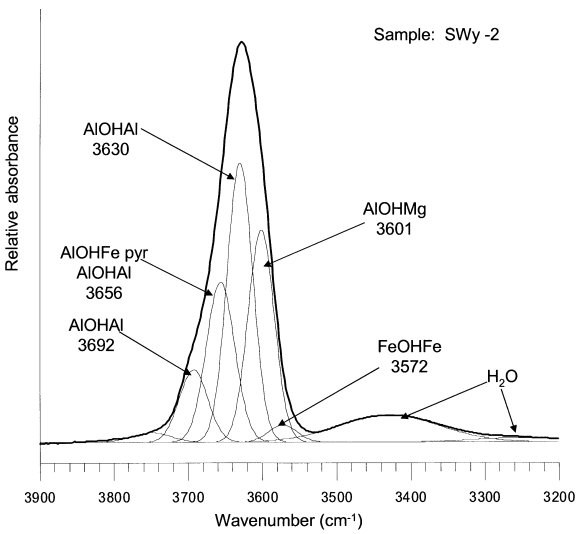

Figure 5. Decomposition of the IR spectrum of Fe-rich montmorillonite SWy-2.

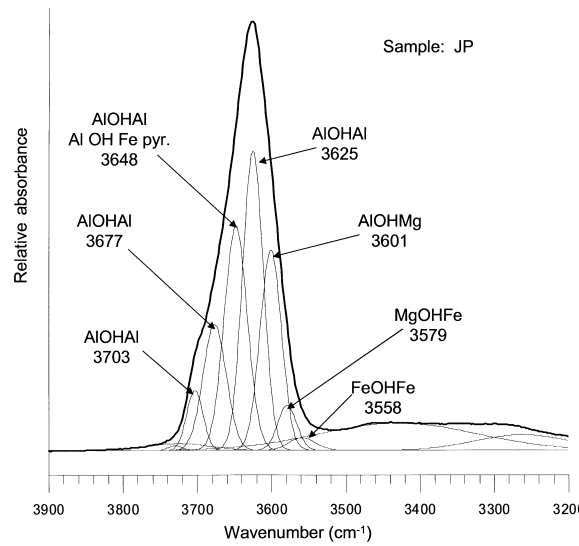

Figure 6. Decomposition of the IR spectrum of Fe-rich montmorillonite Jelsovy Potok (JP).

https://doi.org/10.1346/CCMN.2004.0520401 Published online by Cambridge University Press

Table 4. Mean positions of OH-stretching bands corresponding to specific cation pairs for dioctahedral micas and smectites.

Band	Mica*	Smectite†	e.s.d.‡
$Fe^{2+}OHFe^{2+}$	3505		
$Fe^{2+}OHFe^{3+}$	3521		
$Fe^{3+}OHFe^{3+}$	3535	3538	4
$Fe^{3+}OHFe^{3+}$		3556	5
$Fe^{3+}OHFe^{3+}$		3573	5
$MgOHFe^{3+}$	3559	3580	1
$AlOHFe^{3+}$	3573	3593	4
MgOHMg	3583	3588	3
AlOHMg	3604	3607	4
AlOHAl	3621	3628	4
AlOHAl	3641	3652	4
AlOHAl	3658		
pyr.-like $AlOHFe^{3+}$	3652	3653	5
AlOHAl	3675	3673	4
AlOHAl		3693	5

* Besson and Drits (1997a)
† This work
‡ estimated standard deviations for OH-band positions in smectite spectra (cm^{-1})

1–5 cm^{-1}). In several cases, the band position variation ranges overlap: AlOHFe (3586–3595 cm^{-1}) and MgOHMg (3585–3591 cm^{-1}); AlOHAl (3644–3657 cm^{-1}) and AlOHFe of the pyrophyllite-like component (3648–3660). Thus, the final criterion for correct assignment of the OH-band positions in a spectrum is the agreement between the octahedral cation compositions calculated from the IR data with that given by the crystal-chemical formula.

Table 5 shows that the octahedral cation compositions of the studied smectite samples obtained from the relative integrated intensities of the corresponding bands are in good agreement with the crystal-chemical formulae (the discrepancies are 0–0.07 atoms per $O_{10}(OH)_2$).

DISCUSSION

Molecular water absorption

There has been considerable ambiguity as to the number and positions of the spectral components in the complex molecular water band of dioctahedral 2:1 phyllosilicates. This band overlaps on its high-frequency side with the structural OH-stretching vibrations. Farmer (1974) suggested that in the IR spectra of smectites, this complex H_2O band consisted of a broad band near 3400 cm^{-1}, a shoulder at 3250 cm^{-1} (interpreted as an overtone of water-bending vibration at 1630 cm^{-1}), and a narrow band at 3610–3630 cm^{-1}. Madejová *et al.* (1994), who decomposed IR spectra of three smectite samples, fitted the residual water absorption with two broad bands at 3410 and 3500 cm^{-1} and a narrow band at 3650 cm^{-1}. In the IR spectra of dioctahedral micas, Besson and Drits (1997a) fitted the molecular water band with two broad maxima at 3260 and 3420 cm^{-1} corresponding to two types of structurally connected water. Fialips *et al.* (2002a), in a study of the IR spectra of reduced Garfield nontronite with varied Fe^{2+}/Fe^{3+} ratios, approximated the molecular water absorption with two broad bands at 3415–3485 cm^{-1} and 3205–3285 cm^{-1} and a narrow band at 3590 cm^{-1} that was identified only in the case of reduced nontronite samples. Similar results were reported for Al-rich nontronite SWa-1b (Fialips *et al.*, 2002b).

In the present study, the molecular water absorption was approximated with two broad bands at 3185–3262 cm^{-1} (mean value = 3227 cm^{-1}) and at 3425–3440 cm^{-1} (mean value = 3431 cm^{-1}) (Table 2). The third high-frequency band was not found in any of

Table 5. Octahedral cation compositions of the studied smectites (atoms per $O_{10}(OH)_2$) obtained from chemical analysis (c.a.) data and calculated from relative integrated intensities of OH-stretching bands.

		Al		Fe		Mg	
	Sample	c.a.	IR	c.a.	IR	c.a.	IR
1	BJ 1.98	1.96	0.02	0.04			
2	BT 1.87	1.80	0.09	0.13	0.04	0.07	
3	Otay	1.18	1.25	0.08	0.05	0.74	0.70
4	Polkville	1.42	1.41	0.08	0.11	0.50	0.48
5	Montmorillon	1.65	1.70	0.04	0.03	0.30	0.27
6	SAz-1	1.36	1.39	0.08	0.05	0.56	0.56
7	598	0.35	0.30	1.68	1.70		
8	1092	0.33	0.32	1.60	1.60	0.07	0.08
9	SWa-1a	0.64	0.62	1.22	1.25	0.14	0.13
10	SWa-1b	0.54	0.54	1.34	1.33	0.12	0.13
11	SWy-2	1.54	1.49	0.23	0.23	0.24	0.28
12	BF 1.58	1.56	0.20	0.24	0.22	0.19	
13	JP 1.57	1.58	0.17	0.17	0.26	0.25	
14	2M5	1.50	1.54	0.16	0.15	0.35	0.31

https://doi.org/10.1346/CCMN.2004.0520401 Published online by Cambridge University Press

the spectra; this may be associated with the small amount of residual water in the studied samples.

Cation-OH-cation vibrations

General regularities. Qualitatively, in the IR spectra of dioctahedral smectites, the distribution of the stretching bands corresponding to different cation environments of OH groups follow the same regularities as found by Besson and Drits (1997b) for dioctahedral micas. (1) For cations with similar or identical atomic masses, an increase in the sum of valencies for the cation pair leads to an increase in the wavenumber of the corresponding band; (2) for the same sum of valencies of the OH-bonded pair of cations, an increasing sum of cation masses decreases the wavenumber of the corresponding band. There are, however, certain differences between the number and positions of the individual cation-OH-cation bands in mica and smectite spectra.

Table 4 shows that the band positions of specific OH-bonded cation pairs in the spectra of smectites are generally shifted to greater wavenumbers with respect to those in dioctahedral micas. One of the possible reasons for this shift may be associated with the different orientation of the OH vector. In dioctahedral micas, the OH vector is tilted towards the vacant octahedron and forms a minor angle with the *ab* plane (from 15º in muscovite to 0º in celadonite) one of the main reasons being the repulsion between the hydroxyl proton and the interlayer cation. As a result, the proton forms hydrogen bonds with two apical oxygen atoms in the octahedral sheet, which weakens the bonding within the OH group (Besson and Drits, 1997b). In a dehydrated smectite interlayer, the interlayer cation, as well as an isolated residual H_2O molecule, can be located exactly above the ditrigonal cavity in the tetrahedral sheet. Therefore, because of low interlayer cation occupancy, the OH vector should form a significantly larger angle with the *ab* plane, so that the hydrogen bonds between the hydroxyl proton and the apical oxygens are probably much weaker. This may account for the relative strengthening of the OH bond that leads to the increase in wavenumber for individual OH-stretching bands. It remains unclear, however, why the shift in wavenumber is greater for vibrations that involve Fe than for AlOHAl, AlOHMg and MgOHMg bands. For example, the positions of the $AlOHFe^{3+}$ band in the mica and smectite IR spectra are 3573 and 3593 cm^{-1}, respectively, whereas the positions of the AlOHMg band are fairly close: 3604 (3601–3610 cm^{-1}) for micas and 3607 (3601–3613) cm^{-1} for smectites (Table 4). Further investigation will be needed to gain a deeper insight into this problem.

FeOHFe vibrations. Besson and Drits (1997a, 1997b) found three FeOHFe-stretching bands in the spectra of dioctahedral micas: $Fe^{2+}OHFe^{2+}$, $Fe^{2+}OHFe^{3+}$ and $Fe^{3+}OHFe^{3+}$ (Table 4). In the IR spectra of dioctahedral smectites, we have identified, depending on the samples' chemical composition, from one to three FeOHFe-stretching bands at ~3538, 3556 and 3573 cm^{-1} (Tables 2, 4), assuming them all to refer to trivalent Fe. In a few cases, a fourth band of low intensity appeared in the FeOHFe region at ~3500–3510 cm^{-1}. The fourth band could be an artifact resulting from the assumption of strictly Gaussian peak shape in the curve-fitting procedure.

The presence of two or more often three, FeOHFe-stretching bands in the spectra of Fe-rich smectites may result from differences in the environment around the Fe cations and the OH group. Specifically, the tetrahedra located close to a hydroxyl proton may be occupied by either Si or Al leading to differences in the effective charge on the apical oxygens shared by the tetrahedra and octahedra and in the repulsion between the hydroxyl proton and the tetrahedral cation, which would affect the strength of the hydrogen bond formed by the proton and the apical oxygen and consequently, the bonding within the OH group (Besson and Drits, 1997b). Similarly, the bond strength in the OH group will depend on whether the interlayer site at the ditrigonal cavity nearest to the hydroxyl proton in the dehydrated layer is vacant or occupied. If this interlayer site is occupied by Na or Ca, repulsion between the interlayer cation and the hydroxyl proton would weaken the O–H bonding; the presence of a residual water molecule with its O atom attracting the hydroxyl proton would strengthen the bond within the OH group. The combination of these factors may lead to the appearance of more than one FeOHFe-stretching band in the IR spectra.

Our data on the positions of the FeOHFe bands partly coincide with those available in the literature. Madejová *et al*. (1994) reported two FeOHFe bands for Al-rich nontronite SWa-1b at 3532 and 3554 cm^{-1}. Fialips *et al*. (2002a) identified two FeOHFe bands in the spectrum of unaltered Garfield nontronite at 3532 and 3572 cm^{-1} and suggested several alternative explanations for the 3532 cm^{-1} band. For an unaltered SWa-1b sample, Fialips *et al*. (2002b) suggested one FeOHFe band at 3565 cm^{-1}. The IR spectra decomposition results of Fialips *et al*. (2002a, 2002b), however, appear questionable because in both papers the Gaussian-Lorentzian mixing ratios for the band shape were left variable and "were automatically determined" by the curve-fitting procedure.

AlOHAl- and AlOHMg-stretching vibrations. In dioctahedral micas, Besson and Drits (1997a) recognized three bands corresponding to AlOHAl-stretching vibrations of the mica structure: at 3621, 3641 and 3658 cm^{-1}. Gates (2003) found three distinct AlOHAl bands in the IR combination spectra of dioctahedral smectites**.** In the present study, we have identified two AlOHAl-stretching bands around 3628 and 3652 cm^{-1} (Tables 2, 4). The presence of several bands assigned to AlOHAl may be

https://doi.org/10.1346/CCMN.2004.0520401 Published online by Cambridge University Press

associated with a combination of various structural effects. For example, Al for Si substitutions in tetrahedra adjacent to the OH-sharing Al octahedra should lead to an increase in wavenumber of the AlOHAl band, whereas Mg for Al substitutions in the adjacent octahedra would cause a decrease (Besson and Drits, 1997b). The actual positions of the AlOHAl bands may be also be affected by the nearest interlayer site being either occupied or vacant (see above). According to calculations of the samples' chemical compositions from the IR data, the bands at 3673 and 3693 cm^{-1} should also be attributed to AlOHAl but they probably refer to pyrophyllite-like structural fragments within the smectite structure (see below). Our data differ from those of Madejová *et al.* (1994) who identified two AlOHAl bands, at 3618 and 3635 cm^{-1}, for smectites SWy-1, JP and SWa-1b.

For SWy-1 and JP, Madejová *et al*. (1994) attributed to AlOHMg not only the band at ~3600 cm^{-1}, but also, following Farmer (1974), to that at ~3680 cm^{-1}. In the present work, only one AlOHMg band around 3607 cm^{-1} was identified, both for these two samples and for the other smectites. In the present study, no band at 3680 cm^{-1} was found for SWy-1 (Figure 5, Table 2), and in the case of JP the band at 3678 cm^{-1} was assigned to AlOHAl of the pyrophyllite-like component (Figure 6, Table 2).

The MgOHMg band. Quantum mechanical calculations of structural models of dioctahedral phyllosilicates in the illite-smectite series (Sainz-Diaz *et al*., 2002) showed that Mg cations tend to be dispersed in the octahedral sheet in contrast to Fe cations that have a tendency to cluster. Experimental studies by Cuadros *et al.* (1999) and Sainz-Diaz *et al.* (2001) using IR spectroscopy in the OH-bending region also did not reveal MgMg pairs in the octahedral sheets of bentonitic illite-smectite. On the contrary, Besson and Drits (1997a) found MgOHMg-stretching bands in the IR spectra of Mg-rich dioctahedral micas. In a recent study of clay minerals at the Cretaceous/Tertiary boundary in Denmark (Drits *et al.*, 2004), the strong band at 3585 cm^{-1} in the IR spectrum of montmorillonite HSI was attributed to the MgOHMg-stretching vibration. Indirect but strong theoretical and experimental evidence for the existence of Mg-OH-Mg cations in dioctahedral smectites was obtained by Méring and Glaeser (1954). These authors showed that different proportions of interlayer Ca cations should be required to provide local compensation of the 2:1 layer negative charge originating from Mg-OH-Mg pairs in *trans*-vacant (*tv*) and *cis*-vacant (*cv*) montmorillonites containing the same amount of randomly distributed octahedral Mg (Fe^{2+}) and Al (Fe^{3+}) cations. If the occurrence probability for Mg (Fe^{2+}) to replace Al (Fe^{3+}) in an octahedral site is p, then $4p$ is the number of Mg (Fe^{2+}) per $O_{20}(OH)_4$. A simple theoretical consideration given by Méring and Glaeser (1954) shows that in the case of *tv* montmorillonites, the proportion α of interlayer Ca cations necessary for local compensation of the Mg-OH-Mg negative charge should be equal to p. In contrast, for *cv* montmorillonite, the α value should be significantly higher and equal to $2p/(1+p)$. In agreement with the theoretical prediction, it was found experimentally that $\alpha = 0.333$ for montmorillonite from Camp-Berteau for which, according to the structural formula, $p = 0.2$. Accordingly, this *cv* montmorillonite has a proportion of Mg-OH-Mg cationic pairs equal to that corresponding to random distribution of octahedral di- and trivalent cations.

The MgOHMg band was also identified in the spectra of four of the montmorillonites studied in this work (Otay (#3), Polkville (#4), Montmorillon (#5), and SAz-1 (#6), Table 2). This is the only way to attribute the strong band at ~3588 cm^{-1}, which is present along with the AlOHMg and AlOHAl bands in these spectra. Indeed, these samples have relatively high Mg contents (from 0.3 to 0.74 atoms per $O_{10}(OH)_2$) and low Fe and there are no other cation configurations that would account for it. The cation compositions of these samples calculated from the IR data with this band assignment are in excellent agreement with those given by the crystal-chemical formulae (Table 5).

Pyrophyllite-like structural fragments. According to Besson and Drits (1997a), dioctahedral mica structures having a deficiency of interlayer cations may contain pyrophyllite-like structural fragments. Tsipursky (pers. comm.) observed pyrophyllite-like domains in mica structures using high-resolution transmission electron microscopy. In the IR spectra of several celadonites, glauconites and illites, the bands at 3652 and 3675 cm^{-1} were attributed to AlOHFe- and AlOHAl-stretching vibrations, respectively, that refer to pyrophyllite-like local environments. These values are very close to the positions of the AlOHFe- (3647 cm^{-1}) and AlOHAl- (3675 cm^{-1}) stretching bands in pyrophyllite IR spectra (Farmer, 1974; Besson and Drits, 1997a). The heating and dehydration under vacuum of the smectite samples in combination with small contents of interlayer cations may have led to the formation of pyrophyllite-like structural environments on an even wider scale than in micas. This is confirmed by the analysis of the IR data. The large amount of Fe in sample SWa-1b and the relatively high Fe contents in samples SWy-2, BF, JP and 2M-5 can be quantitatively accounted for only if the band at 3648–3660 cm^{-1} (mean = 3653 cm^{-1}) is attributed to the AlOHFe vibration of the pyrophyllite-like component. Moreover, most of the studied samples having high Al contents show OH-stretching bands at ~3673 and/or 3693 cm^{-1} (Table 2). These bands were identified as AlOHAl vibrations of the pyrophyllite-like component, although the origin of the band at 3693 cm^{-1} remains somewhat problematic. The position of the band at 3673 cm^{-1} agrees well with that of AlOHAl both in pure pyrophyllite (Farmer, 1974) and in

https://doi.org/10.1346/CCMN.2004.0520401 Published online by Cambridge University Press

pyrophyllite-like local fragments in micas (Besson and Drits, 1997a). The high intensity of this band in beidellite BJ (Tables 2, 4) may be associated with the coexistence of extensive pyrophyllite-like domains and domains of beidellite having higher Al-for-Si substitution than in the average crystal-chemical formula.

Short-range order/disorder in the octahedral cation distribution

The good agreement that has been obtained between the results of spectra decomposition and crystal-chemical formulae for a large collection of dioctahedral smectites of diverse compositions implies that for monomineral samples with known chemical compositions, IR data can provide information on the short-range order/disorder in the distribution of octahedral cations along cation-OH-cation directions. This information can be derived from the comparison of the relative intensities of the individual bands corresponding to different types of OH-bonded cations with those expected for a random cation distribution. Taking account of the possible ambiguity in the decomposition of unresolved spectra, discrepancies between these experimental and theoretical values should be regarded as significant when they exceed 15–20% of relative integrated intensity.

Figure 7 shows the experimental total relative areas of AlOHAl bands (which are equivalent to occurrence probabilities of OH-bonded Al-Al pairs) plotted as a function of the theoretical areas that would be observed in the case of a random distribution of octahedral cations in each sample. The individual points for most of the samples plot along the 1:1 line, which means that the occurrence probabilities of AlAl pairs along the cation-OH-cation directions, are close to those expected for a random cation distribution. In sample SWy-2, the amount of OH-bonded AlAl pairs is significantly less than would be in the case of random cation distribution. The points for Mg-rich and Fe-free montmorillonites (Otay, SAz-1, Polkville, Montmorillon) lying above the 1:1 line may indicate an increased tendency to formation of AlOHAl pairs.

Figure 8 shows that the amount of OH-bonded AlMg pairs in Mg-rich montmorillonites (Polkville, SAz-1, Otay) is significantly less than expected for random cation distribution. This is in agreement with the increased formation of MgOHMg pairs observed for these samples. On the contrary, Fe-rich montmorillonites JP and SWy-2 seem to show a tendency to ordered alternation of Al and Mg along the cation-OH-cation direction.

The experimental relative areas of FeOHFe bands in the studied nontronites and Fe-rich montmorillonites plot along the 1:1 line (Figure 9). An increased tendency to Fe segregation, however, may be noted for sample SWa-1a.

Figure 10 shows that the number of OH-linked AlFe pairs in samples SWa-1a and SWa-1b is significantly smaller than expected for random cation distribution, which is in agreement with a tendency to Fe segregation.

In all three samples where the MgOHFe band was identified (BF, JP and 2M5), the relative abundance of this grouping is greater than expected for random octahedral cation distribution (Figure 11).

Analysis of Figures 7–11 shows that smectite samples having similar cation compositions (*e.g.* SWy-2, BF and JP) and even different fractions of the same heterogeneous sample (SWa-1a and SWa-1b) can

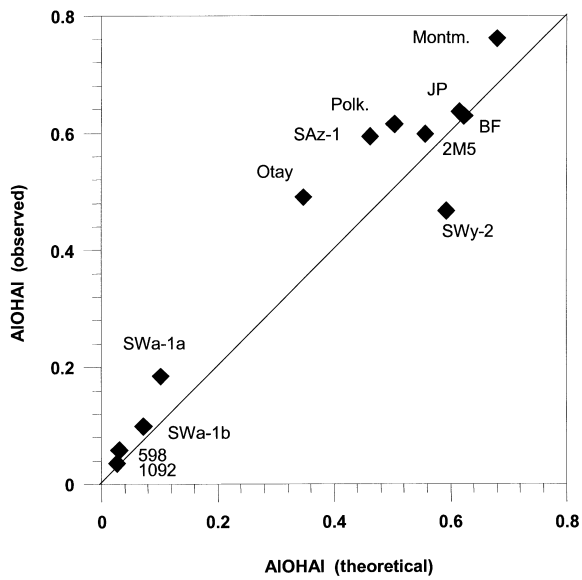

Figure 7. Experimental occurrence probabilities of OH-bonded AlAl pairs as a function of theoretical occurrence probabilities calculated for statistical cation distribution.

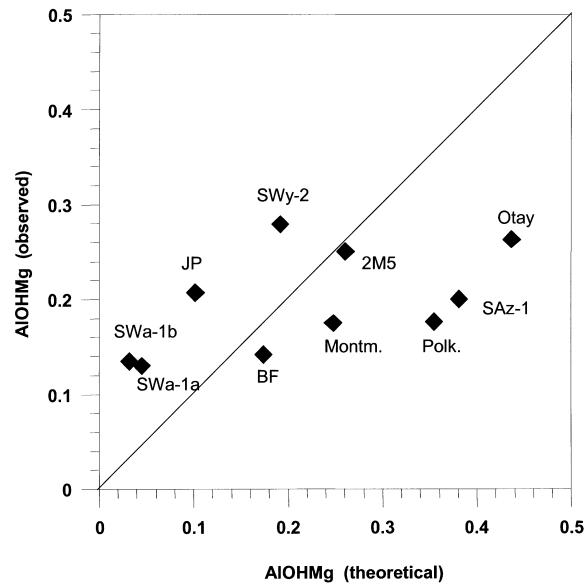

Figure 8. Experimental occurrence probabilities of OH-bonded AlMg pairs as a function of theoretical occurrence probabilities calculated for statistical cation distribution.

https://doi.org/10.1346/CCMN.2004.0520401 Published online by Cambridge University Press

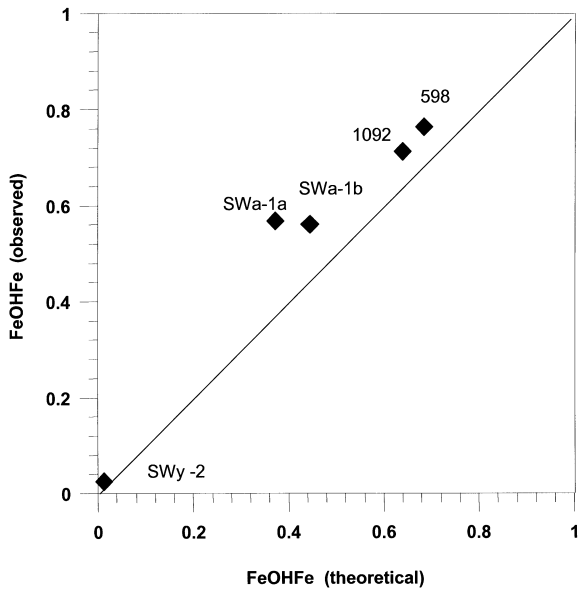

Figure 9. Experimental occurrence probabilities of OH-bonded FeFe pairs as a function of theoretical occurrence probabilities calculated for statistical cation distribution.

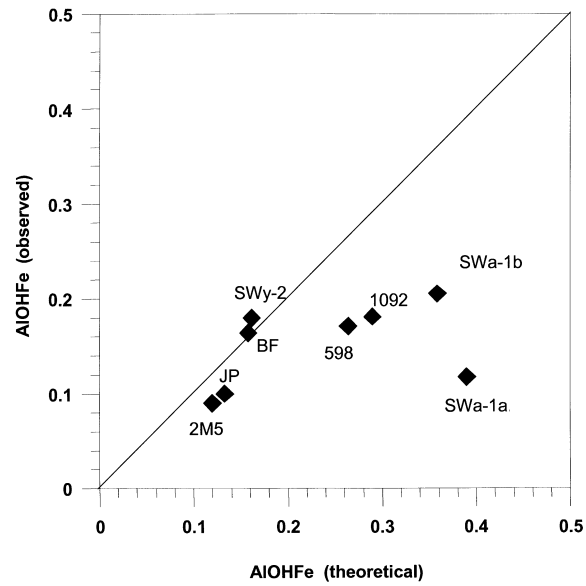

Figure 10. Experimental occurrence probabilities of OH-bonded AlFe pairs as a function of theoretical occurrence probabilities calculated for statistical cation distribution.

differ in the short-range order/disorder in the octahedral cation distribution.

Because of the differences in the spectra decomposition and band assignments, it is difficult to compare the peculiarities in octahedral cation distribution revealed for samples SWy-2, JP and SWa-1 in this work with the results of Madejová *et al*. (1994). On a qualitative level, however, some of the inferences coincide. The greater (as compared to random distribution) probability of OH-linked MgFe pairs in JP; the nearly random distribution of Al and Fe along the cation-OH-cation direction in SWy-2; the distributions of AlAl, FeFe, AlMg and AlFe cation pairs are similar in SWa-1 (Madejová *et al*., 1994) and SWa-1b (of the two samples SWa-1a and SWa-1b, the cation composition of the latter is closer to that of SWa-1 studied by Madejová *et al*. (1994) and Vantelon *et al*. (2001) and is nearly identical to that of Manceau *et al*., 2001).

Manceau *et al*. (2001), who studied several reference nontronites by EXAFS, found that, in SWa-1, the number of Fe-Fe and Fe-Al(Mg) pairs, when averaged over the three crystallographic directions, follow statistical distribution. With account taken of the data obtained in the present work, this may imply that the Fe-Fe pairs are preferentially aligned along the *b* direction, whereas Fe-Al(Mg) pairs are aligned along the directions oriented at ±120º with respect to *b*.

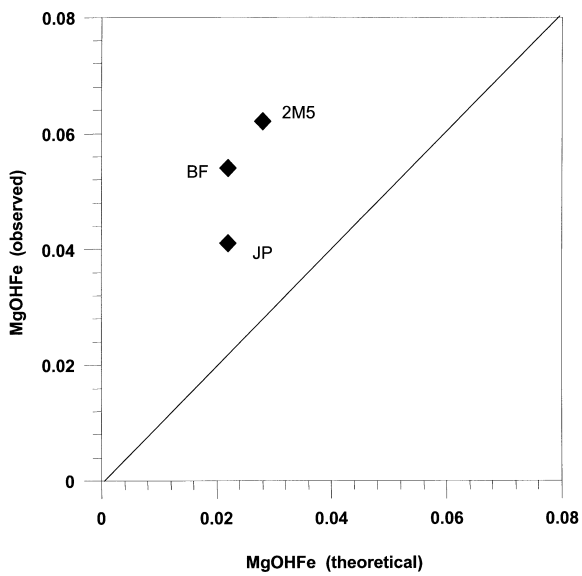

Figure 11. Experimental occurrence probabilities of OH-bonded MgFe pairs as a function of theoretical occurrence probabilities calculated for statistical cation distribution.

CONCLUSIONS

Decomposition and curve-fitting of IR spectra applied to a representative collection of dioctahedral smectites provided a crystal-chemically consistent assignment of individual OH-stretching bands to specific types of OH-bonded cation pairs. The poor resolution of the individual bands in smectite IR spectra, however, may lead to several decompositions that would describe the experimental spectrum equally well. This ambiguity was minimized by using a unique set of individual OH-band positions to describe the IR spectra for a large number of smectites of diverse compositions. Reliable interpretation of the OH-stretching vibrations in smectite IR spectra is therefore possible only for samples with known chemical compositions. This also means that IR data cannot be used for

https://doi.org/10.1346/CCMN.2004.0520401 Published online by Cambridge University Press

quantitative determination of octahedral cation composition of mixtures of dioctahedral 2:1 phyllosilicates. On the other hand, for monomineral smectites with known chemical compositions, IR data may provide information on the short-range order/disorder in the distribution of octahedral cations along cation-OH-cation directions. This information can be employed, in combination with the data of other spectroscopic and diffraction techniques, in the analysis of two-dimensional octahedral cation distribution (Dainyak *et al*., 1992; Drits *et al*., 1997; Dainyak and Kheifits, 1999; Cuadros *et al*., 1999; Manceau *et al*., 2001; Sainz-Diaz *et al*., 2001).

ACKNOWLEDGMENTS

The authors are grateful to Drs S. Petit and W. Gates for valuable comments and suggestions. C. Ignacio Sainz-Diaz also deserves thanks for valuable comments. Thanks are due to Russell Anderson of ChevronTexaco for his help with the experimental part of the work. V.A. Drits is grateful to ChevronTexaco for financial support. V.A. Drits and B.B. Zviagina acknowledge the financial support of the Russian Foundation for Fundamental Research (RFFI), grant 01-05-64486.

REFERENCES

Besson, G. and Drits, V.A. (1997a) Refined relationships between chemical composition of dioctahedral fine-dispersed mica minerals and their infrared spectra in the OH stretching region. Part I. Identification of the stretching bands. *Clays and Clay Minerals*, **45**, 158–169.

Besson, G. and Drits, V.A. (1997b) Refined relationship between chemical composition of dioctahedral fine-dispersed mica minerals and their infrared spectra in the OH stretching region. Part II. The main factors affecting OH vibration and quantitative analysis. *Clays and Clay Minerals*, **45**, 170–183.

Chekin, S.S. (1973) *Lower Mesozoic Weathering Crust of Irkutsk Region.* Nauka, Moscow, 155 pp. (in Russian).

Čičel, B. and Komadel, P. (1994) Structural formulae of layer silicates. Pp. 114–136 in: *Quantitative Methods in Soil Mineralogy* (J.M. Bartels, editor). Soil Science Society of America, Madison, Wisconsin.

Cuadros, J. and Altaner, S.P. (1998) Compositional and structural features of the octahedral sheet in mixed-layer illite-smectite from bentonites. *European Journal of Mineralogy*, **10**, 111–124.

Cuadros, J., Sainz-Diaz, C.I., Ramirez, R. and Hernandez-Laguna, A. (1999) Analysis of Fe segregation in the octahedral sheet of bentonitic illite-smectite by means of FTIR, ^{27}Al MAS NMR and reverse Monte-Carlo simulations. *American Journal of Science*, **299**, 289–308.

Dainyak, L.G. and Kheifits, L.M. (1999) The improved equation for the Fe^{3+} quadrupole doublet assignment and computer simulation of cation distribution in trans-vacant dioctahedral micas. *EUROCLAY 1999 program with Abstracts*, p. 72. Institute of Geological Sciences PAN, Krakow.

Dainyak, L.G., Drits, V.A. and Heifits, L.M. (1992) Computer simulation of cation distribution in dioctahedral 2.1 layer silicates using IR data. Application to Mössbauer spectroscopy of a glauconite sample. *Clays and Clay Minerals*, **40**, 470–479.

Decarreau, A., Grauby, O. and Petit, S. (1992) The actual distribution of octahedral cations in 2:1 clay minerals: results from clay synthesis. *Applied Clay Science*, **7**, 147–167.

Drits, V.A., Dainyak, L.G., Muller, F., Besson, G. and Manceau, A. (1997) Isomorphous cation distribution in celadonites, glauconites, and Fe-illites determined by infrared, Mössbauer and EXAFS spectroscopies. *Clay Minerals*, **32**, 153–179.

Drits, V.A., Lindgreen, H., Sakharov, B.A., Jakobsen, H.J and Zviagina, B.B. (2004) The structure and origin of clay minerals at the Cretaceous/Tertiary Boundary, Stevns Klint (Denmark). *Clay Minerals* (in press).

Eberl, D.D., Środoń, J. and Northrop, H.R. (1986) Potassium fixation in smectite wetting and drying. Pp. 296–326 in: *Geochemical Processes at Mineral Surfaces* (J.A. Davis and K.F. Hayes, editors). ACS Symposium Series, **323**, American Chemical Society.

Farmer, V.C. (1974) The layer silicates. Pp. 331–363 in: *Infrared Spectra of Minerals* (V.C. Farmer, editor). Monograph **4**, Mineralogical Society, London.

Farmer, V.C. and Russell, J.D. (1964) The infrared spectra of layer silicates. *Spectrochimica Acta*, **20**, 1149–1173.

Fialips, C.I., Huo, D., Yan, L., Wu, J. and Stucki, J.W. (2002a) Effect of Fe oxidation state on the IR spectra of Garfield nontronite. *American Mineralogist*, **87**, 630–641.

Fialips, C.I., Huo, D., Yan, L., Wu, J. and Stucki, J.W. (2002b) Infrared study of reduced and reduced-reoxidized ferruginous smectite. *Clays and Clay Minerals*, **50**, 45–469.

Foster, M.D. (1953) Geochemical studies of clay minerals. II Relation between ionic substitution and swelling in montmorillonite. *American Mineralogist*, **38**, 994–1006.

Gates, W.P. (2003) Infrared spectroscopy and the chemistry of dioctahedral smectites. In: *Vibrational Spectroscopy of Layer Silicates and Hydroxides* (T. Kloprogge, editor). Clay Minerals Society Workshop Series, **14**, Boulder (in press).

Gates, W.P., Slade, P.G., Manceau, A. and Lanson, B. (2002) Site occupancies by iron in nontronite. *Clays and Clay Minerals*, **50**, 223–239.

Jackson, M.L. (1985) *Soil Chemical Analysis – Advanced Course.* Published by the author, Madison, Wisconsin, 895 pp.

Madejová, J., Putyera, K. and Čičel, B. (1992) Proportion of central atoms in octahedral layers of smectites calculated from IR spectra. *Geologica Carpathica Series Clays*, **43**, 117–120.

Madejová, J., Komadel, P. and Čičel, B. (1994) Infrared study of octahedral site populations in smectites. *Clay Minerals*, **29**, 319–326.

Manceau, A., Lanson, B., Drits, V.A., Chateigner, D., Gates, W.P., Wu, J., Huo, D. and Stucki, J.W. (2001) Oxidation-reduction mechanism of iron in dioctahedral smectites: 1. Crystal chemistry of oxidized reference nontronites. *American Mineralogist*, **85**, 133–152.

McCarty, D.K. and Reynolds, R.C., Jr. (1995) Rotationally disordered illite-smectite in Paleozoic K-bentonites. *Clays and Clay Minerals*, **43**, 271–284.

Méring, J. and Glaeser, R. (1954) Sur le rôle de la valence des cations échangeables dans la montmorillonite. *Bulletin de la Société Française de Minéralogie et Cristallographie*, **77**, 519–530.

Petit, S., Robert, J.L., Decarreau, A., Besson, G., Grauby, O. and Martin, F. (1995) Contribution of spectroscopic methods to 2:1 clay characterization. Pp. 119–147 in: *Structure et Transformation des Argiles dans les Champs Pétroliers et Géochimiques.* Elf-Aquitaine Production, **19**.

Petit, S., Caillaud, J., Righi, D., Madejová, J., Elsass, F. and Köster, H.M. (2002) Characterization and crystal chemistry of an Fe-rich montmorillonite from Ölberg, Germany. *Clay Minerals*, **37,** 283–297.

Russell, J.D. and Fraser A.R. (1994) Infrared methods. Pp. 11–67 in: *Clay Mineralogy: Spectroscopic and Chemical*

https://doi.org/10.1346/CCMN.2004.0520401 Published online by Cambridge University Press

Determinative Methods (M.J. Wilson, editor). Chapman & Hall, London.

Sainz-Diaz, C.I., Cuadros, J. and Hernandez-Laguna, A. (2001) Analysis of cation distribution in the octahedral sheet of dioctahedral 2.1 phyllosilicates by using inverse Monte Carlo methods. *Physics and Chemistry of Minerals*, **28**, 445–454.

Sainz-Diaz, C.I., Timon, V., Botella, V., Artacho, E. and Hernandez-Laguna, A. (2002) Quantum mechanical calculations of dioctahedral 2:1 phyllosilicates: Effect of octahedral cation distributions in pyrophyllite, illite and smectite. *American Mineralogist*, **87**, 958–965.

Slonimskaya, M.V., Besson, G., Dainyak, L.G., Tchoubar, C. and Drits, V.A. (1986) The interpretation of the IR spectra of celadonites and glauconites in the region of the OH stretching frequencies. *Clay Minerals*, **21**, 377–388.

Środoń, J., Morgan, D.J., Eslinger, E.V., Eberl, D.D. and Karlinger, M.R. (1986) Chemistry of illite-smectite and end-member illite. *Clays and Clay Minerals*, **34**, 368–378.

Strens, R.G. Jr. (1974) The common chain, ribbon and ring silicates. Pp. 305–330 in: *Infrared Spectra of Minerals* (V.C. Farmer, editor). Monograph **4**, Mineralogical Society, London.

Vantelon, D., Pelletier, M., Michot, L.J., Barres, O. and Thomas, F. (2001) Fe, Mg and Al distribution in the octahedral sheet of montmorillonites. An infrared study in the OH-bending region. *Clay Minerals*, **36**, 369–379.

(*Received 6 November 2003; revised 15 March 2004; Ms. 853*)

https://doi.org/10.1346/CCMN.2004.0520401 Published online by Cambridge University Press